

Magnetic properties and ^{119}Sn hyperfine interactions investigated in RCoSn (R=Tb, Dy, Ho, Er) compounds

This article has been downloaded from IOPscience. Please scroll down to see the full text article.

1994 J. Phys.: Condens. Matter 6 11127

(<http://iopscience.iop.org/0953-8984/6/50/020>)

View [the table of contents for this issue](#), or go to the [journal homepage](#) for more

Download details:

IP Address: 171.66.16.179

The article was downloaded on 13/05/2010 at 11:35

Please note that [terms and conditions apply](#).

Magnetic properties and ^{119}Sn hyperfine interactions investigated in RCoSn ($\text{R} = \text{Tb}, \text{Dy}, \text{Ho}, \text{Er}$) compounds

E A Görlich†, R Kmieć‡, K Łątka†, A Szytuła† and A Zygmunt§

† Institute of Physics, Jagiellonian University, 30-059 Kraków, Poland

‡ Institute of Nuclear Physics, Kraków, Poland

§ Institute of Low-Temperature and Structural Research, Wrocław, Poland

Received 9 May 1994, in final form 29 September 1994

Abstract. It was confirmed that samples of RCoSn ($\text{R} = \text{Tb}, \text{Dy}, \text{Ho}, \text{and Er}$) compounds have the orthorhombic NiTiSi -type structure. They all order antiferromagnetically with transition temperatures T_N decreasing along the series: 20.5 K, 10 K, 7.8 K, and 4 K, respectively. Their complex non-collinear magnetic structures result in a multicomponent appearance of the Mössbauer spectra recorded for 23.8 keV γ -transition of ^{119}Sn at temperatures below T_N . In the case of DyCoSn the hyperfine-split spectra are observed above T_N due to the non-vanishing transferred fields at the tin sites in the paramagnetic state. A change in the type of magnetic ordering of TbCoSn at 11.6 K may be inferred from both magnetic and Mössbauer measurements. Mean values of the saturation transferred hyperfine fields at tin nuclei scale roughly with the square root of magnetic transition temperatures T_N .

1. Introduction

The ternary intermetallic compounds containing rare-earth and d transition elements have been subjects of intensive studies due to their interesting physical properties [1–3]. The family of compounds described by the formula RTX (where $\text{R} =$ rare earth, $\text{T} =$ transition metal, and $\text{X} = \text{Si}, \text{Ge}, \text{Al}, \text{Ga}, \text{As}, \text{In}, \text{and Sn}$) is one of the many classes of ternary intermetallic compounds which are known to exist [3]. Compounds of this family form structures of different types such as the cubic (LaIrSn , MgAgAs type), the hexagonal (CaIn_2 , Fe_2P , Ni_2In type), the tetragonal (LaPtSi , PbFCl type), and the orthorhombic (NiTiSi , CeCu_2 type) [4]. Among them the compounds with tin as an X element have drawn much attention in particular with respect to the heavy-fermion, Kondo-lattice and related phenomena encountered in Ce-, Eu-, Sm-, or Yb-containing phases [5–9]. The sustained and ever-growing interest in *anomalous* lanthanide behaviours over the last two decades requires a thorough and well documented knowledge of systems based on *normal* i.e. well and stably localized 4f rare-earth elements. In the search for phenomenological correlations between physical properties we have concentrated on a systematic investigation of a small subgroup of the latter compounds retaining the same structure namely that of the NiTiSi type. X-ray diffraction data indicate that RCoSn ($\text{R} = \text{Tb}, \text{Dy}, \text{Ho}, \text{and Er}$) compounds crystallize with such an orthorhombic lattice. The magnetic susceptibility of these compounds (for $\text{R} = \text{Tb–Lu}$) in the temperature range 78–300 K roughly obeys the Curie–Weiss law [10]. In this paper we present and discuss the results of the x-ray, magnetic, and ^{119}Sn Mössbauer-effect measurements for the four members of the RCoSn family viz. with $\text{R} = \text{Tb}, \text{Dy}, \text{Ho}, \text{and Er}$. Information acquired from these methods was successfully

reconciled with the picture emerging from the neutron-diffraction experiments reported in [11] and [12].

2. Experimental details

The RCoSn (R = Tb, Dy, Ho, and Er) were prepared by the arc melting of the stoichiometric amounts of the constituent elements (of purity 3N for rare-earth elements and 4N for Co and Sn) in an inert atmosphere of argon gas. Afterwards the samples were annealed at 800 °C for one week. Powder x-ray diffraction studies were performed using DRON-3 diffractometer equipped with a Co K α radiation source. The Foner-type magnetometer was used for magnetic measurements in the temperature range of 4.2 K–300 K and a magnetic field of up to 50 kOe.

The investigations of the hyperfine interactions of ^{119}Sn nuclei were carried out by means of the Mössbauer effect in the temperature range from 1.9 K to 300 K. The source used had the chemical form of barium stannate and all the values of the isomer shift further quoted are given relative to this material at room temperature. Special attention was paid to assuring *the thin-absorber condition* so that thickness effects hardly played a role in the observed broadening of spectra at low temperatures (cf. e.g. [13]).

Table 1. Crystallographic and magnetic data for RCoSn (R = Tb, Dy, Ho, and Er) compounds.

Compound	a (Å)	b (Å)	c (Å)	T_N (K)	Θ_p (K)	μ_{eff} (μ_B)	μ_{th}^a	Reference
TbCoSn	7.154(5)	4.558(4)	7.470(8)	20.5	+ 15(5)	9.8(1)	9.72	This work
	7.260(5)	4.534(2)	7.348(2)		+ 30	9.77		[10]
DyCoSn	7.156(5)	4.546(2)	7.474(6)	10	+ 9(4)	10.5(1)	10.63	This work
	7.202(3)	4.526(4)	7.448(4)		+ 27	10.43		[10]
HoCoSn	7.138(8)	4.517(5)	7.469(7)	7.8	+ 7(3)	10.4(2)	10.61	This work
	7.154(5)	4.503(4)	7.461(7)		+ 9	10.47		[10]
ErCoSn	7.101(8)	4.496(5)	7.446(9)	~4	0(4)	9.6(1)	9.58	This work
	7.093(8)	4.486(4)	7.431(6)		+ 11	9.42		[10]

$$^a \mu_{\text{th}}(\text{R}^{3+}) \equiv g\sqrt{J(J+1)}.$$

3. Results

The x-ray and the earlier neutron-diffraction data [12] indicate that the studied compounds possess an orthorhombic NiTiSi-type structure at room temperature. The lattice parameters of these compounds as obtained from the least-squares fit to the experimental x-ray spectra are given in table 1. They approximately agree with the values of [10]. The magnetization curves are shown in figure 1 and a change in the slope of the low-field portion of the μ against H dependence at about $H_c = 4$ kOe suggests the occurrence of the metamagnetic or spin-flop phase transition in the studied compounds except, perhaps, ErCoSn. In all cases the magnetization attained at 4.2 K in fields up to 50 kOe is far from the full saturation theoretical value. The temperature dependence of the magnetization at the applied field of $H = 10$ kOe indicates no phase transition and the reciprocal magnetic susceptibility generally follows the Curie–Weiss law (figure 2). The determined values of the paramagnetic Curie temperatures and the effective magnetic moments are listed in table 1. The measurements at magnetic field below H_c give the Néel temperature $T_N = 20.5$ K for TbCoSn and $T_N = 10$ K for DyCoSn (inset of figure 2). For TbCoSn an additional phase transition below T_N is observed

at 11.6 K (figure 3). The antiferromagnetic transition temperatures for HoCoSn and ErCoSn were found to be equal to 7.8 K and 4 K, respectively.

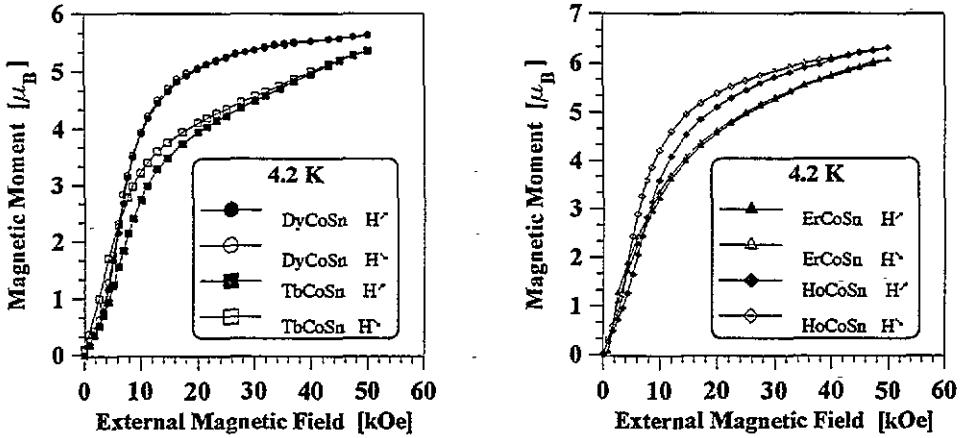


Figure 1. Magnetization per formula unit as a function of the applied magnetic field at $T = 4.2$ K is shown for TbCoSn, DyCoSn, HoCoSn, and ErCoSn.

Gamma resonant-absorption spectra show the hyperfine patterns for all four samples at low temperatures. The values of the ^{119}Sn isomer shifts are indicative of the proximity of the electronic structure of tin in these compounds to the divalent state (table 2). The electric quadrupole coupling constant (EQCP) defined as $\frac{1}{4}e^2qQ$ measures the energy associated with an interaction of the nuclear quadrupole moment eq and the surrounding charge distribution (given by the main component of an electric field gradient eQ).

Table 2. Selected parameters of the ^{119}Sn Mössbauer absorption spectra for RCoSn (R = Tb, Dy, Ho, and Er) compounds.

Compound	B_{hf} (T) at 1.9 K	IS^a (mm s $^{-1}$) at 1.9 K	IS (mm s $^{-1}$) at RT	EQCP (mm s $^{-1}$) at RT
TbCoSn	6.43	1.70(2)	1.72(1)	0.28(1)
DyCoSn	4.55	1.68(2)	1.71(1)	0.27(1)
HoCoSn	2.31	1.71(2)	1.72(1)	0.28(1)
ErCoSn	1.50	1.72(2)	1.72(1)	0.30(1)

^a Averaged value weighted by components' relative intensities.

The interaction of the tin nuclear magnetic moment leading to the observed splitting of the spectrum may be described as a coupling to the local hyperfine field (B_{hf}). This field acting at the sites of tin nuclei is of a transferred character i.e. originates from the rare-earth localized 4f moments and is mediated by the polarization of a conduction band by means of the RKKY-type mechanism. The first remarkable feature of the Mössbauer spectra common to all samples at low temperatures (i.e. below T_N) is the presence of a few hyperfine components characterized by a set of discrete values of the hyperfine fields (figure 4). The spectra were consistently (for different temperatures and for all samples) fitted with theoretical curves under the assumption of a few distinct subspectra. In all samples there is a single *low-field* component (i.e. with a small value of B_{hf}) and a group of the remaining constituent subspectra of distinctly larger fields. Figure 5 shows the temperature

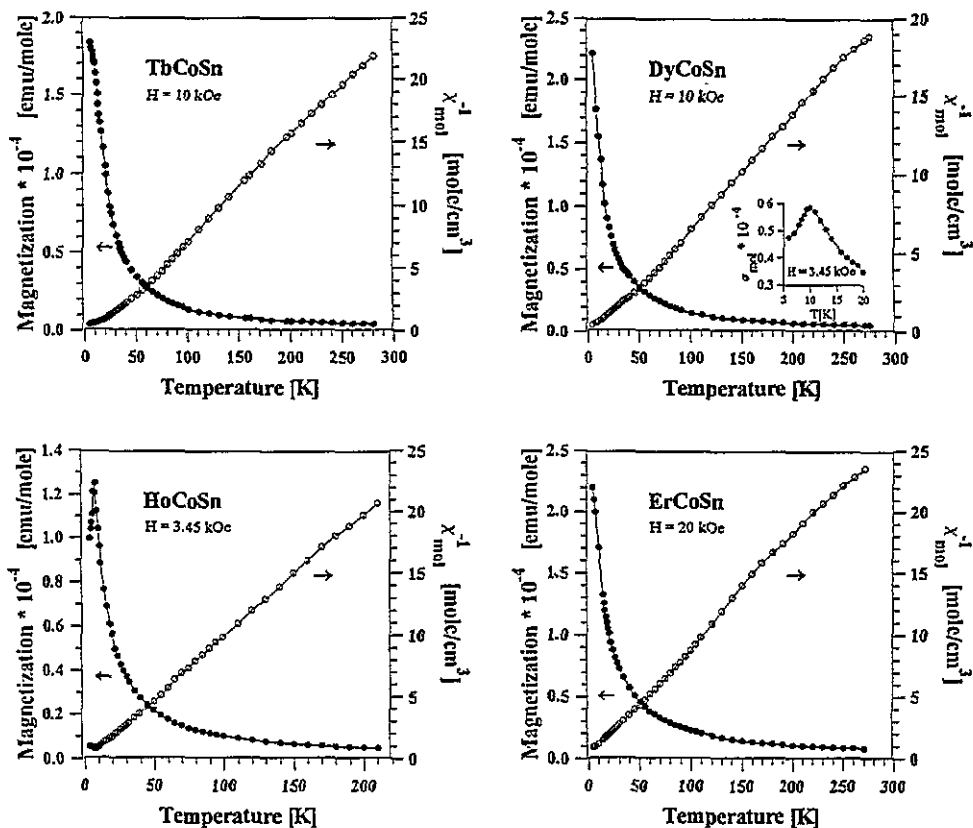


Figure 2. Temperature dependence of the molar magnetization and reciprocal molar magnetic susceptibility of TbCoSn and DyCoSn at $H = 10$ kOe, of HoCoSn at $H = 3.45$ kOe, and of ErCoSn at $H = 20$ kOe. The inset presents the magnetization curve for DyCoSn at $H = 3.45$ kOe in the vicinity of the antiferromagnetic transition.

evolution of an average field value calculated according to $\bar{B}_{\text{hf}} = \sum_{i=1}^N p_i B_i(\text{Sn})$, where p_i is a relative contribution to the spectrum intensity from the i th component and N is the respective number of these components in a given sample (a bar denotes here and in what follows the site-averaged value). The number N of subspectra is the smallest set of components to reproduce experimental data satisfactorily. The value of N was established to be equal to five for TbCoSn, four in the case of DyCoSn, and three for the low-temperature spectra of Ho and Er compounds. These numbers later found full support in the respective configurations of magnetic moments as determined by the neutron-diffraction studies [12], and this is discussed below. Furthermore, the temperature variation of the hyperfine field $\bar{B}_{\text{hf}}(\text{Sn})$ shows that this quantity does not vanish at the bulk magnetic critical temperature T_N . The effect is particularly pronounced for the DyCoSn compound and is hardly present in the case of TbCoSn. No abrupt qualitative change in the character of the spectrum of the former compound is observed upon increasing the temperature above T_N (figure 8). This means that the basic features of the magnetic structure survive, on the local scale as probed by the Mössbauer effect, to temperatures considerably higher than T_N . The mean hyperfine field \bar{B}_{hf} gradually decreases with increasing temperature, and eventually the resulting broadening of the spectrum ceases to be observable at about 35 K (figure 5).

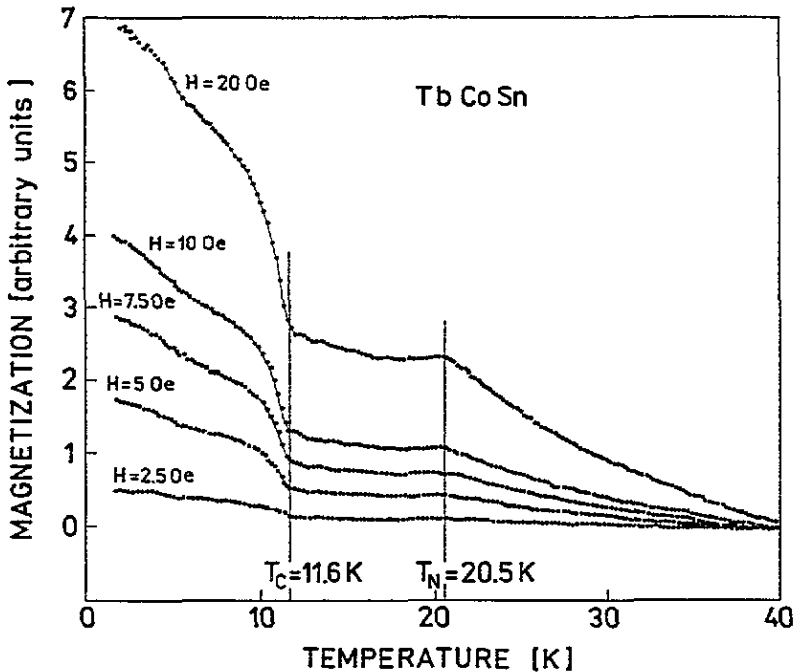


Figure 3. Temperature dependence of the magnetization at low applied magnetic fields for TbCoSn.

4. Discussion

RCoSn compounds crystallize in the orthorhombic structure of NiTiSi type with the $Pnma$ space group. All component atoms of RCoSn occupy four available (c) sites each, characterized by a mirror plane $b = \frac{1}{4}$ as the only non-trivial symmetry element. Figure 6 shows the spatial arrangement of atoms surrounding a certain tin atom in the unit cell of HoCoSn (as an example). It is formed by atoms belonging to the three adjacent $b = -\frac{1}{4}$, $b = \frac{1}{4}$, and $b = \frac{3}{4}$ planes. The tin coordination polyhedron is highly irregular. In consequence the interatomic distances show variety. The values quoted below were calculated using the atomic positions obtained by neutron diffraction [12]. Two cobalt atoms are present near the Sn atom within the (c, a) plane (inset of figure 6); one of them is distinctly further from the tin (3.10 Å) than the other (2.33 Å). The next two cobalt atoms in the nearest vicinity of tin remain at equal distances $d_{Co-Sn} = 2.46$ Å but belong to the neighbouring parallel planes. The observed distances are smaller than the sum of the covalent radii of cobalt and tin atoms, which indicates a strong chemical interaction. The rare-earth atoms form wavy chains running along the a axis with large R-R separation (e.g. for Ho: 3.64 Å). The chains form mirror planes normal to the b axis with intersection parameter $y = \frac{1}{4}$ and $\frac{3}{4}$. The antiphase relative position of rare-earth chains of the adjacent planes creates two values of R-R distances between their atoms. For HoCoSn they are 3.82 Å and 4.91 Å. This particular feature of a variety of R-R distances between neighbouring rare-earth ions allows us to expect the occurrence of a more complex magnetic structure. In view of the single crystallographic position taken by the tin ions in these compounds (4(c)) the reason for a multicomponent form of the γ -absorption spectra in a magnetically ordered state must be a complex spin arrangement. This leads to a number of distinct tin nuclei

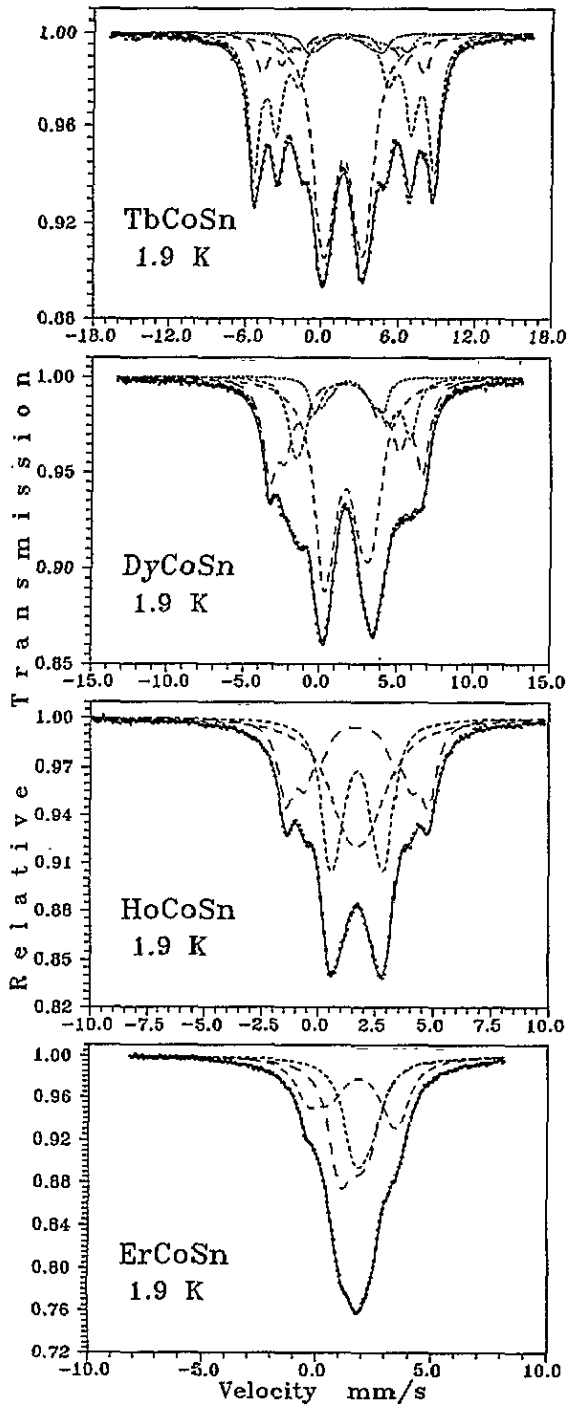


Figure 4. Mössbauer spectra of ^{119}Sn in TbCoSn, DyCoSn, HoCoSn, and ErCoSn at 1.9 K.

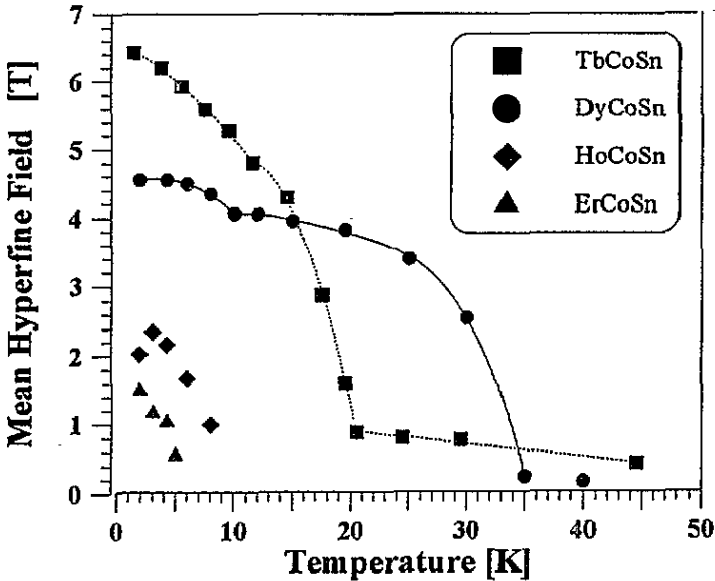


Figure 5. Temperature evolution of the mean hyperfine splitting as observed for ^{119}Sn nuclei by means of the Mössbauer effect for TbCoSn, DyCoSn, HoCoSn, and ErCoSn.

environments. Recent neutron-diffraction measurements [12] brought a nice confirmation of the above assumption, and it reveals reasons for the qualitative similarity of the low-temperature spectra of all samples. The moments remain in the (b, c) plane taking two, symmetrical inclinations with respect to the b axis. Generally, the magnetic structures of these four compounds differ in a period of a square-modulated antiferromagnetic lattice. Additionally a tilting angle within the (b, c) plane differs between the compounds. Figure 7 shows dysprosium magnetic moment configurations around tin ions encountered in the antiferromagnetic state of DyCoSn. These four environments explain the four-component form of the hyperfine-split Mössbauer spectrum (figure 8). In this compound the relative abundance of each type of tin-atom neighbourhood is $a:b:c:d \Leftrightarrow 4:1:1:1$, which reasonably agrees with the relative intensities of the spectral components. In the case of TbCoSn the change in the antiferromagnetic structure found at 11.6 K in magnetization measurements reported here and observed in neutron experiments [12] is reflected in the contributions to the Mössbauer spectrum from the different components (figure 9). The period of HoCoSn magnetic structure is shorter and allows for three types of local tin environments—exactly the number of hyperfine components observed in the Mössbauer spectrum. Moreover, their relative intensities 1:1:1 agree with the frequency of occurrence of each site. Overall hyperfine splitting in the γ -resonance spectra of ErCoSn is small and does not allow the reliable recognition of all four components which might have been expected on the basis of magnetic structure. On the other hand, the tilting angle of the Er moment to the b axis is exceedingly small and therefore the differentiation of site environments is not very pronounced. In this case an overlap of two components may well occur. The situation described here may be contrasted with those encountered in SmAgSn [8], and in TbPdSn [5] where the simple antiferromagnetic structure results in a single-component ^{119}Sn Mössbauer spectra.

Magnetization against temperature measurements performed for TbCoSn at low applied

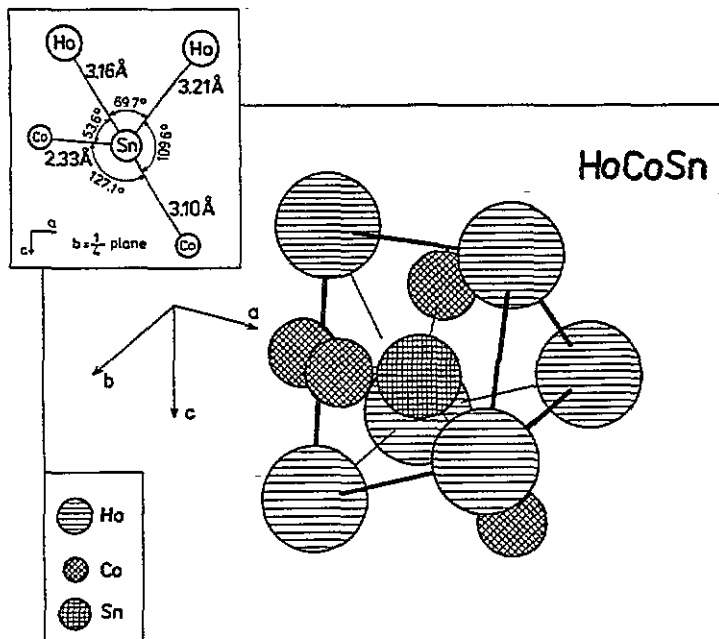


Figure 6. Nearest neighbourhood of the tin ion in the structure of HoCoSn. The inset shows the atomic arrangement in the central $b = \frac{1}{4}$ plane of the main picture. The distances and angles were based on the atomic positions obtained from the room-temperature neutron reference data.

fields (figure 3) show its special softness. The reason may lie in a subtle balance between the factors determining the actual spin arrangement: the long-range RKKY coupling and the crystal-field interaction of the trivalent rare-earth ions. The cobalt atoms do not carry a localized magnetic moment in these compounds. Closer inspection of the mean hyperfine-field against temperature plot for TbCoSn (figure 5) allows us to notice at temperatures of 11.6 K and 20.5 K the features marking a reorganization of the Tb magnetic moment arrangement. The first (lower) temperature marks (albeit very subtly) the change in the type of antiferromagnetic ordering as may also be inferred from magnetization against temperature measurements performed at various external magnetic fields (figure 3). The higher of the singular temperatures separates antiferromagnetic and paramagnetic states. The residual hyperfine interactions of the tin nuclei, only slowly vanishing with temperature, result in a 'tail' in the \bar{B}_{hf} against T plot (figure 5). The effect is due to incomplete averaging out of the local magnetic field at Sn sites in the paramagnetic state. The Néel temperature of DyCoSn is 10.5 K (cf. table 1) and it is clearly marked by a change in the slope of the temperature dependence of $\bar{B}_{\text{hf}}(\text{Sn})$ at the tin site. The residual field above T_N (as averaged over all spectral components) shows only a small reduction in value with respect to the field measured close to magnetic saturation while in the case of TbCoSn the local correlations above T_N show up in a mere broadening of the absorption line. It is evident from the neutron results [12] that at temperatures above T_N the orientation of the rare-earth magnetic moments lacks the spatial coherence over the sample volume i.e. no long-range order is present. The exchange coupling between the neighbouring spins tends to align them. The non-vanishing spin-spin correlation function for the nearest rare-earth neighbourhood of a given tin atom is equivalent to the magnetic ordering persisting on a local scale. One may talk about the

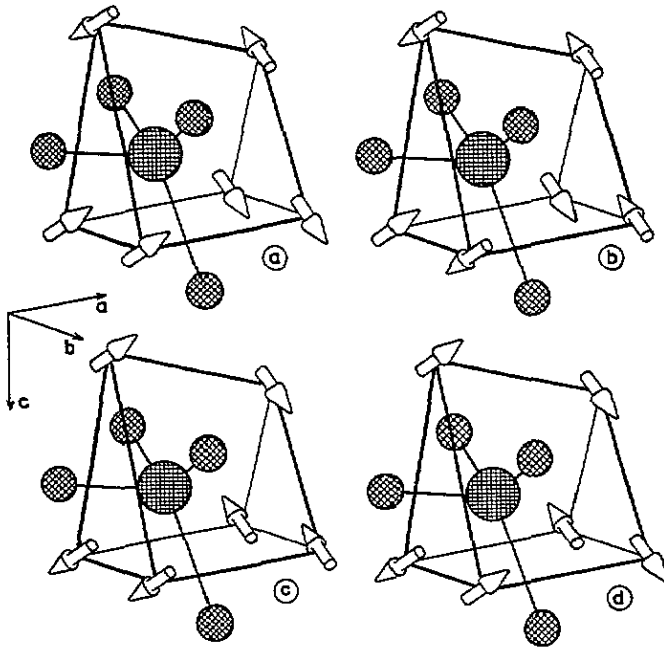


Figure 7. Four types of rare-earth magnetic moment's arrangement in the nearest neighbourhood of tin in DyCoSn at temperatures below T_N . According to the neutron-scattering results the moments remain in the (b, c) plane.

magnetic clusters which should be understood as the dynamical entities rather than domains enforced by a particular atomic arrangement. The picture is conceptually analogous to the idea of dynamical clusters evoked in [14] to describe the formation of regions of low- and high-temperature phases in the vicinity of the structural phase transition. The spatial correlations are probably short ranged, say of the order of several lattice constants, and temperature dependent. These correlations are subject to time fluctuations. The necessary condition for the observation of the non-zero transferred hyperfine field at the tin nuclei is a slow enough time evolution of the correlation function. The time scale is set by the time resolution of the ^{119}Sn Mössbauer spectroscopy, and is determined by the period of the Larmor precession of a nuclear moment in a local field, i.e. of the order of $\nu_L^{-1} = 10^{-8}$ s (the estimation for ^{119}Sn in $B_{\text{hf}} = 1$ T). The spin correlations, both in space and time, are suppressed by the increasing temperature leading to the observed \bar{B}_{hf} against T dependence (figure 5). The effects described above are responsible for the overestimation of the Néel temperature of ErCoSn from the $\bar{B}_{\text{hf}}(\text{Sn})$ against T dependence (figure 5) with respect to the magnetic data.

The systematics of the bulk magnetic transition temperatures of the investigated compounds generally follows the tendency expected from the de Gennes relation (figure 10). The proportionality of transition temperature T_N to $G \equiv (g_J - 1)^2 J(J + 1)$ stems from the underlying RKKY mechanism of the magnetic indirect coupling. Undoubtedly, the crystal-field interactions are one of the important factors contributing to the observed deviations. There are, however, basic reasons which make the linear dependence of T_N on G much of a phenomenological character, especially in the case of antiferromagnetics of complex structures. According to the RKKY approach T_N depends on the details of crystal,

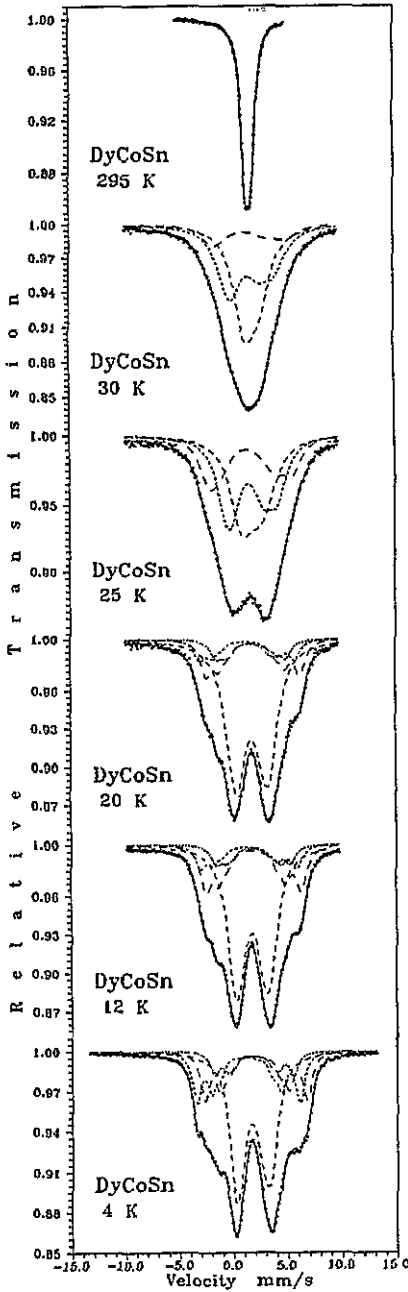


Figure 8. The temperature evolution of the ^{119}Sn Mössbauer spectrum of DyCoSn at $T = 295$ K, 30 K, 25 K, 20 K, 12 K and 4 K.

magnetic, and electronic structures (e.g. [17]):

$$T_N = -\frac{3\pi Z^2}{k_B E_F} \Omega^{-2} J_{sf}^2 (g_J - 1)^2 J(J+1) \sum_{i \neq 0} F(2k_F \cdot R_i) f(Q \cdot R_i)$$

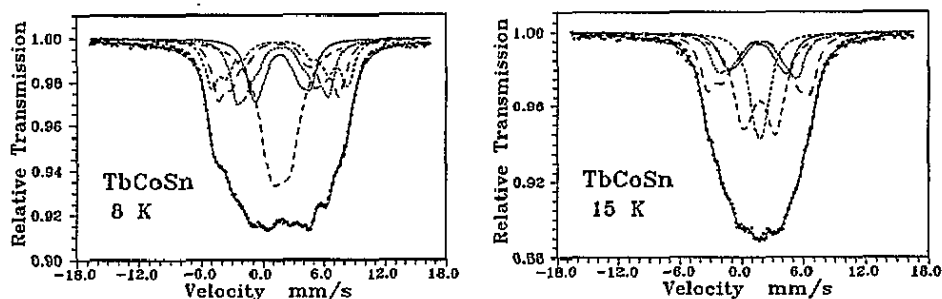


Figure 9. A change in the antiferromagnetic structure which takes place at 11.6 K is reflected in the change of splittings and intensities of the components in the TbCoSn ^{119}Sn Mössbauer spectra shown here at $T = 8$ K and 15 K.

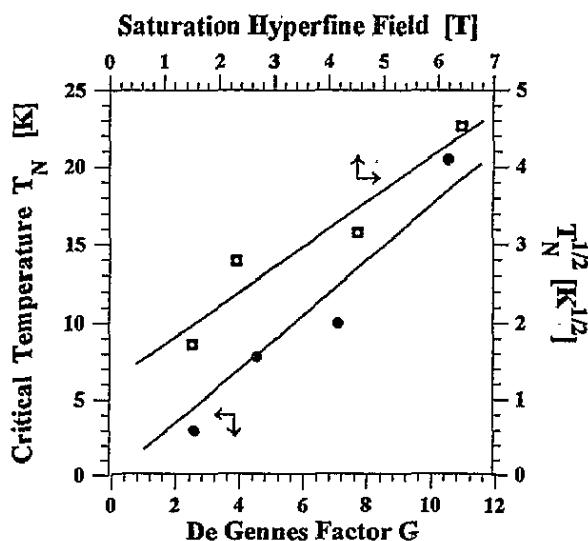


Figure 10. Comparison of the restricted RKKY model predictions with experimental data for RCoSn compounds: (a) the Néel temperature T_N against de Gennes factor $G \equiv (g_J - 1)^2 J(J+1)$, (b) saturation hyperfine field at ^{119}Sn sites \bar{B}_{hf} against square root of the Néel temperature.

where the oscillatory function $F(2k_F \cdot R_i)$ has the form $F(x) = (x \cos(x) - \sin(x))/x^4$. The relevant parameters are the conduction- f -electron exchange integral J_{sf} (with the wave-vector dependence dropped out), energy E_F and the wave vector k_F at the Fermi surface; the Q wave vector accounts for the particular commensurate magnetic structure via a periodic function f . Z/Ω is the density of conduction electrons. So rather restrictive assumptions are necessary to await a simple linear T_N against G relation. Figure 10 shows also the saturation values of the mean (over all Sn sites) hyperfine field \bar{B}_{hf} plotted against the square root of the respective Néel temperatures for a series of investigated compounds. De Gennes scaling of the magnetic transition temperature with the factor G in a row of isostructural rare-earth intermetallics implies quadratic dependence of T_N on the rare-earth ion's spin. Similarly, an RKKY-type mechanism explains the origin of the *transferred* magnetic field at the tin site predicting a linear relation of $B_{\text{hf}}^{\text{cc}}(\text{Sn})$ to the rare-earth spin ($S_i = (g_J - 1)J$ at R_i)

[16, 15]:

$$B_{\text{hf}}^{\text{ce}} \propto \frac{Z^2}{E_{\text{F}}\Omega^2} J_{\text{st}} \sum_i F(2k_{\text{F}} \cdot R_i) S_i.$$

In this case all the limitations and implicit assumptions mentioned in the above discussion of $T_{\text{N}}(G)$ apply. It turns out that a direct *dipolar* contribution to the magnetic field at the tin site from the neighbouring rare-earth moments ($\mu_i \equiv g_J \mu_{\text{B}} J = S g_J / (g_J - 1)$ in a ground state J)

$$B_{\text{hf}}^{\text{dip}} = \sum_i \left[\frac{3R_i(\mu_i \cdot R_i)}{R_i^5} - \frac{\mu_i}{R_i^3} \right]$$

does not importantly influence the character of the relation.

Therefore, both data presentations in figure 10 have been made from the same standpoint. The Mössbauer effect supplies some arguments encouraging to the above phenomenology. In particular the isomer shifts which are sensitive to the electronic charge density at the nucleus do not differ significantly along the series (table 8), and this implies similarity of the compounds' electronic structures. Moreover the spectra of different compounds of the series show a general resemblance in shape and in their temperature evolution.

5. Conclusions

Below temperatures 20.5, 10, 7.8, and ~ 4 K RCoSn compounds with $R = \text{Tb, Dy, Ho, and Er}$ attain antiferromagnetic order of rare-earth moments, respectively. Relatively complex square-modulated magnetic structures lead to the multicomponent form of the low-temperature Mössbauer spectra. Sensitivity of the nuclear method to the local-environment behaviour allows the observation of a short-range magnetic order above the Néel temperature. The effect is by far most pronounced in the case of DyCoSn compound. The shape of its spectrum remains qualitatively unaffected while increasing the temperature above T_{N} . This suggests that the basic features of the magnetic structure are preserved on the local scale accessible to observation with the Mössbauer effect. From the temperature evolution of the γ -absorption spectrum it may be inferred that in this case at only about 35 K *spin-spin correlations become negligible and the resultant hyperfine field at the tin nuclei vanishes.*

The scaling of the transition temperatures T_{N} with the de Gennes factor was tested. Based on the same philosophy the assumption of the proportionality of the saturation hyperfine field $B_{\text{hf}}^{\text{sat}}(\text{Sn})$ to the square root of the respective T_{N} was compared with the experimental values for the above series of isostructural compounds. In both cases the theoretically predicted tendency is qualitatively confirmed by the measured numbers. Quantitative deviations from this exceedingly simplified model may readily be ascribed firstly to the imposed restrictions and secondly to the neglected crystalline-field interactions.

Acknowledgment

The project was supported in part by Grant No 2-0083-91-01 of the State Committee for Scientific Research in Poland.

References

- [1] Rogl P 1984 *Handbook of Physics and Chemistry of Rare Earths* vol 7, ed K A Gschneidner and L Eyring (Amsterdam: North-Holland) ch 5, p 1
- [2] Szytuła A and Leciejewicz J 1989 *Handbook of Physics and Chemistry of Rare Earths* vol 12, ed K A Gschneidner and L Eyring (Amsterdam: North-Holland) ch 83, p 133
- [3] Szytuła A 1991 *Handbook of Magnetic Materials* vol 6, ed K H J Buschow (Amsterdam: Elsevier) ch 6, p 83
- [4] Hørestreidt E, Engel N, Klepp K, Chabot B and Parthé E 1982 *J. Less-Common Met.* **85** 247
- [5] Sakurai J, Yamaguchi Y, Mibu K and Shinjo T 1990 *J. Magn. Magn. Mater.* **84** 157
- [6] Aliev F G, Moshchalkov V V, Zalyalyutdinov M K, Pak G I, Skolozdra R V, Alekseev P A, Lazukov V N and Sadikov I P 1992 *Physica B* **163** 358
- [7] Routsis Ch D, Yakinthos J K and Gamari-Seale H 1992 *J. Magn. Magn. Mater.* **117** 79
- [8] Adam A, Sakurai J, Yamaguchi Y, Fujiwara H, Mibu K and Shinjo T 1990 *J. Magn. Magn. Mater.* **90 & 91** 544
- [9] Adroja D T and Malik S K 1992 *Phys. Rev. B* **45** 779
- [10] Skolozdra R V, Koretzkaya O E and Gorelenko Yu K 1982 *Ukr. Fiz. Zh.* **27** 263
- [11] Bażela W, Leciejewicz J, Małetka K, Szytuła A and Zygmunt A 1994 *Acta Phys. Pol. A* **85** 859
- [12] Bażela W, Leciejewicz J, Stuesser N, Szytuła A and Zygmunt A 1994 *J. Magn. Magn. Mater.* at press
- [13] Görlich E A 1991 *Proc. XXVI Zakopane School on Physics (Zakopane, 1991)* ed J Stanek and A T Pedziwiatr (Singapore: World Scientific) p 180
- [14] Armstrong R L and Martin C A 1975 *Phys. Rev. Lett.* **35** 294
- [15] Bleaney B 1972 *Magnetic Properties of Rare Earth Metals* ed R J Elliot (New York: Plenum) p 383
- [16] Yosida K 1957 *Phys. Rev.* **106** 893
- [17] Jensen J and Mackintosh A R 1991 *Rare Earth Magnetism: Structures and Excitations* (Oxford: Clarendon) ch 2, p 68